Heliyon

Received:
3 October 2018
Revised:
21 November 2018
Accepted:
8 January 2019

Cite as:
Sumitra N. Mangasuli, Kallappa M. Hosamani, Praveen B. Managutti. Microwave assisted synthesis of coumarin-purine derivatives: An approach to *in vitro* anti-oxidant, DNA cleavage, crystal structure, DFT studies and Hirshfeld surface analysis. Heliyon 5 (2019) e01131. doi: 10.1016/j.heliyon.2019.e01131

Microwave assisted synthesis of coumarin-purine derivatives: An approach to *in vitro* anti-oxidant, DNA cleavage, crystal structure, DFT studies and Hirshfeld surface analysis

Sumitra N. Mangasuli [a], **Kallappa M. Hosamani** [a,*], **Praveen B. Managutti** [b]

[a] *Department of Studies in Chemistry, Karnatak University, Dharwad, 580003, India*

[b] *Department of Studies in Solid State and Structural Chemistry Unit, IISC, Bengaluru, 560012, India*

[*] Corresponding author.

E-mail address: dr_hosamani@yahoo.com (K.M. Hosamani).

Abstract

An easy and efficient microwave-assisted protocol has been developed for the synthesis of coumarin-purine hybrids **(3a-3j).** The newly constructed 1,3-dimethyl-7-((substituted)-2-oxo-2*H*-chromen-4-yl)methyl)-1*H*-purine-2,6(3*H*,7*H*)-dione derivatives were evaluated for their *in vitro* antioxidant activity by DPPH free radical-scavenging ability assay and DNA cleavage by using calf thymus. The compound **3i,** shows the most excellent DPPH scavenging activity with a −OH substitution at C7 of coumarin ring. In addition, the structure of compound **3f,** has been elucidated using single crystal X-ray diffraction technique. Theoretical calculations (DFT) were carried out using Gaussian09 program package and B3LYP correlation function. Full geometry optimization were carried out using 6-311G++(d, p) basis set and the frontier orbital energy were presented. Hirshfeld surface analysis was used for the intermolecular interactions in the crystal structure. The experimental result of the compound **3f** has been compared

https://doi.org/10.1016/j.heliyon.2019.e01131

with the theoretical results and it was found that the experimental data are in a good agreement with the calculated values.

Keywords: Pharmaceutical chemistry, Theoretical chemistry

1. Introduction

Most typical challenges of today's world in constructing the potent organic biomolecules are utilization of least energy, hazardous and expensive solvents minimization [1, 2, 3, 4]. Hence lots of organic reactions have been developed using microwave (MW) for chemical conversions to obtain compounds of chemical applications. Microwave technology is the current thrilling field in green chemistry, broadly classified as microwave-assisted organic synthesis [5]. Hence lots of organic reactions are taking place using microwave (MW) for chemical conversions to obtain compounds of chemical applications, and now thrilling field today in green chemistry, broadly noted to as microwave-assisted organic synthesis [5]. Thus, microwave-assisted organic reactions marks in noticeable improvement in dramatic reduction in reaction time from days and hours to minutes, reduce side reactions, reaction rate enhancement and improving the yield and purity of the organic molecules [6, 7, 8, 9, 10].

Reactive oxygen species (ROS) are formed by aerobic organisms as an unavoidable consequence of cell metabolism. Dietary antioxidants are required to reduce the cumulative effects of oxidative damage due to surplus ROS that remains in our system [11]. These free radicals may oxidize lipids, proteins, or nucleic acids which occur through a chain reaction and may form potentially toxic end products that can lead to aging, cancer, atherosclerosis, and some neurodegenerative disorders such as Alzheimer's and Parkinson's diseases [12]. Therefore, oxidation by free radicals can cause not only deterioration of foodstuffs but also harm living organisms. When free radicals overcome our body's ability to neutralize them, they attack the body itself and disturb the action of cellular DNA. Cells with damaged DNA stagnate and are prone to developing cancer and growths. This kind of damage also accelerates the aging process, diabetes and severely taxing the immune system [13].

The coumarin nucleus, which embodies an α,β-unsaturated lactone motif, is a biologically relevant and highly privileged structure, which is found in numerous natural products and bioactive pharmaceutical compounds [14]. Some authors predicted [15] coumarins and hydroxycoumarins which contain minimum one hydroxyl functional group have shown antioxidant activity, since they are hydrogen/electron donors to free radicals [16]. Coumarin derivatives exhibit vast biological activities such as, anti-tuberculosis, anti-microbial, anti-cancer, anti-inflammatory and anti-HIV agents [17, 18, 19, 20, 21, 22, 23, 24]. They are also key components of

https://doi.org/10.1016/j.heliyon.2019.e01131

flavoring agent for a diverse set of food, such as soft drinks, yogurt, muffins etc. [25]. In particular, umbelliferone **(1)**, esculetin **(2)**, scopoletin **(3)** and quercetin **(4)** were found as potent antioxidant agents (Fig. 1) [26]. On the other hand, purine alkaloids also show oxidative DNA breakage in presence of small biomolecules [27].

Very recently, we reported the antimicrobial and anti-TB activity of coumarin-purine derivatives [28], it was observed that compound **3a** having $-CH_3$ substitution at C6 position of coumarin has shown excellent antimicrobial activity. Similarly, compounds **3a** (C6-CH_3) and **3j** (C6-*tert butyl*) substitutions in the coumarin ring have shown excellent anti-TB activity. Recently, our group designed and synthesized several coumarin derivatives with DNA cleavage studies [29, 30], such as coumarin-thiazoline and coumarin-maltol. These research works motivated us to conduct further investigation of coumarin-purine derivatives such as, microwave synthesis, *in vitro* anti-oxidant, DNA cleavage, Crystal structure, DFT studies and Hirshfeld surface analysis. Bond lengths and bond angles were calculated by using optimized molecular structure. Here, we describe a new versatile tool for selection and to perform simple nucleophilic substitution reactions leading to C-N bridged coumarin-purine hybrids based on reaction condition, with a short reaction time, acutely safe, easy to handle and easy work up without further purification (Fig. 2).

2. Result and discussion

2.1. Chemistry

Reaction of 4-bromomethyl coumarins **(1)** with purine **(2)** in anhydrous potassium carbonate using acetone as solvent afforded 1,3-dimethyl-7-((substituted)-2-oxo-2*H*-chromen-4-yl)methyl)-1*H*-purine-2,6(3*H*,7*H*)-dione hybrids **(3a-3j)**. Based on the results obtained from the experimental, it is clear that the microwave approach demonstrated to be extremely fast, providing excellent yield (90–97%) and the

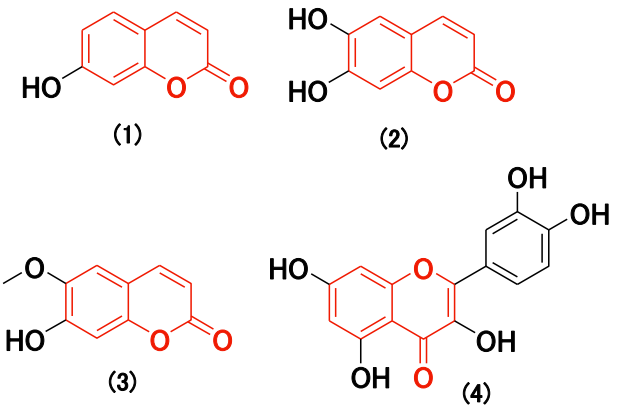

Fig. 1. Structures of the compounds with potent antioxidant activity.

https://doi.org/10.1016/j.heliyon.2019.e01131

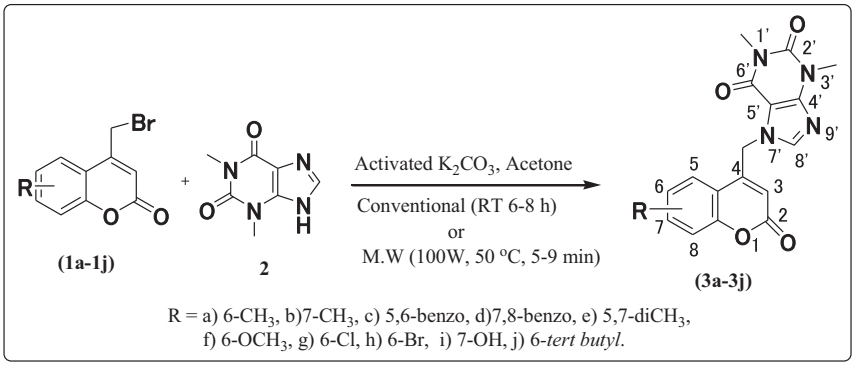

Fig. 2. Schematic representation for the synthesis of the desired compound.

most evident development was the speed with which reaction were completed i.e., within 5−9 minutes, which is provided in Table 1.

2.2. Single crystal X-ray diffraction studies

Single crystal of compound **3f** has been obtained by slow evaporation of chloroform at ambient temperature. Compound **3f** crystallized under a monoclinic system with the space group $P2_1/n$. The unit cell dimensions of compound **3f** are as follows: a = 8.0803(2) Å, b = 13.8722(4) Å, c = 14.7217(4) Å, α = 90°, β = 95.773(2)°, γ = 90°, Z = 4. The dihedral angle of 2*H*-benzo[*h*]chromene ring with the purine ring is 49.68(2)°. In the structure intermolecular C—H…O and weak intramolecular C—H...N & C—H…O hydrogen bonds are observed. The X-ray structure parameters and crystallographic data of compound **3f** are given in Table 2. C-bound H atoms

Table 1. Analytical data of the compounds **(3a-3j)**.

Comp Code	R	Yield		Time	
		[a]C	[b]M	[a]$C_{(h)}$	[b]$M_{(min)}$
3a	6-CH_3	85	97	6.00	5
3b	7-CH_3	84	96	6.00	6
3c	5,6-benzo	80	94	7.00	5
3d	7,8-benzo	83	92	7.50	6
3e	5,7-dimethyl	84	96	7.00	8
3f	6-OCH_3	80	90	7.50	8
3g	6-Cl	75	90	8.00	9
3h	6-Br	73	91	8.00	6
3i	7-OH	74	90	7.50	5
3j	6-*tert butyl*	84	94	6.50	9

[a] **C** − Conventional.
[b] **M** − Microwave.

https://doi.org/10.1016/j.heliyon.2019.e01131

Table 2. Crystal data and structure refinement for compound **3f**.

Identification code	**3f**
Empirical formula	$C_{18}H_{16}N_4O_5$
Formula weight	368.35
Temperature/K	296.15
Crystal system	monoclinic
Space group	$P2_1/n$
a/Å	8.0803(2)
b/Å	13.8722(4)
c/Å	14.7217(4)
α/°	90
β/°	95.773(2)
γ/°	90
Volume/Å^3	1641.81(8)
Z	4
ρ_{calc}g/cm^3	1.490
μ/mm^{-1}	0.112
F(000)	768.0
Crystal size/mm^3	0.25 × 0.23 × 0.21
Radiation	MoKα (λ = 0.71073)
2Θ range for data collection/°	4.044 to 49.988
Index ranges	-9 ≤ h ≤ 9, -16 ≤ k ≤ 11, -17 ≤ l ≤ 17
Reflections collected	13566
Independent reflections	2891 [R_{int} = 0.0229, R_{sigma} = 0.0191]
Data/restraints/parameters	2891/0/247
Goodness-of-fit on F^2	1.078
Final R indexes [I>=2σ (I)]	R_1 = 0.0385, wR_2 = 0.1086
Final R indexes [all data]	R_1 = 0.0464, wR_2 = 0.1135
Largest diff. peak/hole/e Å^{-3}	0.21/-0.20
CCDC No.	**1848347**

were included in calculated positions and treated as riding, with C—H = 0.93–0.97 Å and Uiso(H) = 1.2Ueq(C). The ortep and packing digrams are portrated in Figs. 3 and 4. Theoretical and experimental structural geometry parameters of Bond lengths (A^o) and bond angles (^{o}) for the compound **3f** are summerized in Table 3.

2.2.1. Geometry

All esds (except the esd in the dihedral angle between two least square planes) are estimated using the full covariance matrix. The cell esds are taken into account individually in the estimation of esds in distances, angles and torsion angles; correlations

https://doi.org/10.1016/j.heliyon.2019.e01131

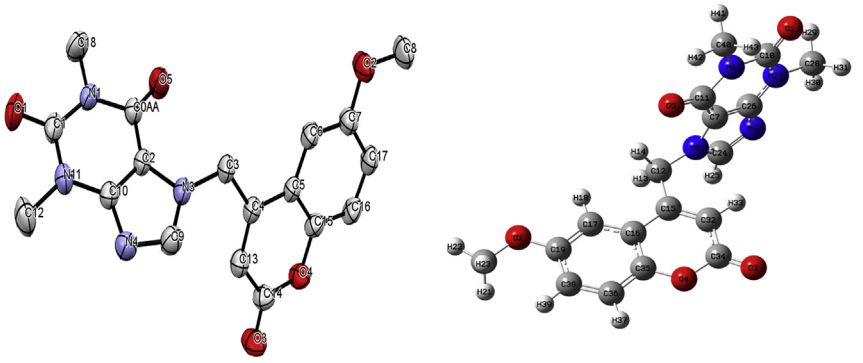

Fig. 3. ORTEP and Optimized structure view of the compound **3f**.

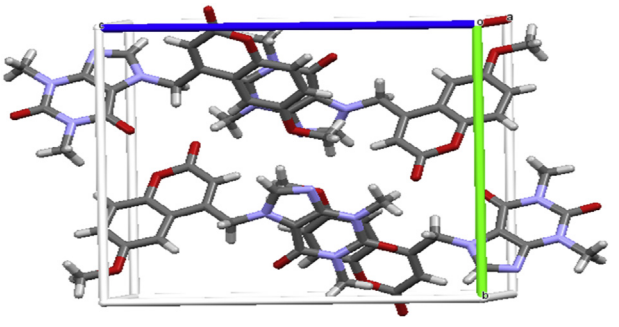

Fig. 4. Packing diagram of the compound **3f**.

between esds in cell parameters are only used when they are defined by crystal symmetry. An approximate (isotropic) treatment of cell esds is used for estimating esds involving least square planes. And refinement on Fractional atomic coordinates and isotropic or equivalent isotropic displacement parameters ($Å^2$) are given Tables 1 and S2 (Available as supplementary material). The crystallographic data is available in [CIF(3f).cif] (Available as supplementary material).

2.3. Frontier molecular orbitals

The results obtained using DFT show that the synthesized compound has the lowest HOMO energy (EHOMO = -6.4795 eV) and the highest LUMO energy (ELUMO = -2.3913 eV). The energy gap (Eg = ELUMO - EHOMO) indicates that the molecule can easily transfer an electron HOMO level to LUMO level. LUMO-HOMO energy gap calculated for the title compound is 4.0882 eV (Fig. 5).

2.4. Hirshfeld surface analysis

Hirshfeld surface analysis is a tool for determining intermolecular interactions that join the molecules in its crystalline arrangement. The intermolecular interactions resolved to the intercontacts between atoms in the crystal structure were quantized

https://doi.org/10.1016/j.heliyon.2019.e01131

Table 3. Theoretical and experimental structural geometry parameters of Bond lengths (A^o) and bond angles (^{o}) for the compound **3f**.

Atom	Length/Å	
	Practical	**DFT calculated**
O1-C1	1.2182(18)	1.217
O2-C7	1.363(2)	1.364
O2-C8	1.418(2)	1.423
O3-C14	1.207(2)	1.204
O4-C14	1.357(2)	1.386
O4-C15	1.383(2)	1.368
O5-C0AA	1.2216(19)	1.225
N1-C1	1.392(2)	1.409
N1-C0AA	1.4053(19)	1.414
N1-C18	1.465(2)	1.469
C2-N3	1.3834(18)	1.390
C2-C0AA	1.416(2)	1.432
C2-C10	1.362(2)	1.379
N3-C3	1.4555(19)	1.458
N3-C9	1.345(2)	1.359
N4-C9	1.321(2)	1.325
N4-C10	1.351(2)	1.360
C1-N11	1.371(2)	1.391
C3-C4	1.504(2)	1.515
C4-C5	1.452(2)	1.455
C4-C13	1.341(2)	1.350
C5-C6	1.395(2)	1.402
C5-C15	1.394(2)	1.407
C6-C7	1.377(2)	1.393
C7-C17	1.392(2)	1.402
C10-N11	1.3705(19)	1.373
N11-C12	1.461(2)	1.465
C13-C14	1.443(2)	1.458
C15-C16	1.374(2)	1.389
C16-C17	1.375(2)	1.390
Bond angle [^{o}]		
C7-O2-C8	117.70(14)	118.7
C14-O4-C15	121.59(12)	122.3
C1-N1-C0AA	126.96(13)	126.7
C1-N1-C18	116.24(13)	115.2
C0AA-N1-C18	116.80(14)	118.1

(*continued on next page*)

https://doi.org/10.1016/j.heliyon.2019.e01131

Table 3. (*Continued*)

Atom	Length/Å	
	Practical	**DFT calculated**
N3-C2-C0AA	132.13(13)	131.2
C10-C2-N3	104.90(13)	105.1
C10-C2-C0AA	122.92(13)	123.6
C2-N3-C3	126.47(13)	126.8
C9-N3-C2	105.47(12)	105.7
C9-N3-C3	127.06(13)	127.4
C9-N4-C10	103.09(13)	104.1
O1-C1-N1	121.60(16)	121.3
O1-C1-N11	121.46(15)	121.5
N11-C1-N1	116.94(13)	117.2
O5-C0AA-N1	121.49(14)	122.6
O5-C0AA-C2	126.98(14)	126.1
N1-C0AA-C2	111.54(13)	111.3
N3-C3-C4	115.20(13)	114.7
C5-C4-C3	116.73(13)	118.2
C13-C4-C3	124.48(14)	122.6
C13-C4-C5	118.76(14)	119.2
C6-C5-C4	124.25(13)	124.2
C15-C5-C4	117.88(14)	117.4
C15-C5-C6	117.85(14)	118.4
C7-C6-C5	120.57(14)	121.0
O2-C7-C6	115.78(14)	115.8
O2-C7-C17	123.93(14)	124.5
C6-C7-C17	120.29(15)	119.7
N4-C9-N3	114.05(14)	113.4
C2-C10-N11	122.08(14)	121.5
N4-C10-C2	112.48(13)	111.6
N4-C10-N11	125.44(14)	126.9
C1-N11-C12	119.59(13)	118.3
C10-N11-C1	119.53(13)	119.7
C10-N11-C12	120.87(15)	122.0
C4-C13-C14	122.78(15)	122.9
O3-C14-O4	117.24(15)	118.3
O3-C14-C13	125.30(16)	125.6
O4-C14-C13	117.46(15)	116.1
O4-C15-C5	121.40(14)	122.0

(*continued on next page*)

https://doi.org/10.1016/j.heliyon.2019.e01131

Table 3. (*Continued*)

Atom	Length/Å	
	Practical	**DFT calculated**
C16-C15-O4	116.80(14)	117.1
C16-C15-C5	121.80(15)	120.9
C15-C16-C17	119.65(15)	120.1
C16-C17-C7	119.81(14)	120.0

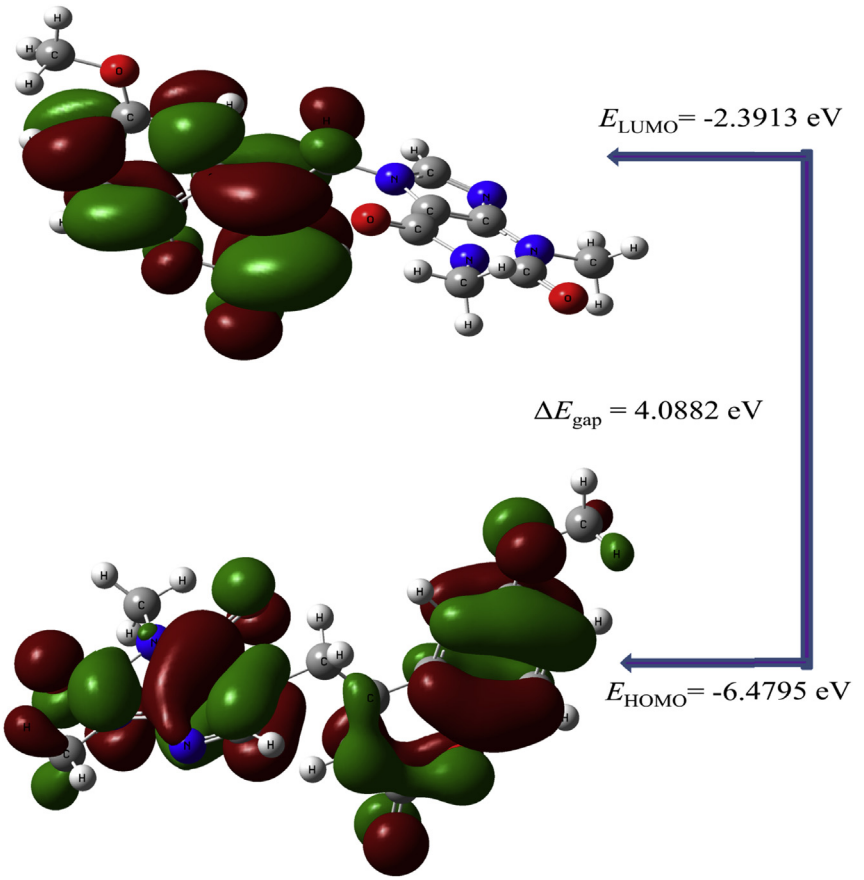

Fig. 5. HOMO and LUMO energy plot of the compound **3f**.

using Hirshfeld surfaces computational analyses (Fig. 6). The electrostatic potential surfaces are plotted (Fig. 7) with red region, which is a negative electrostatic potential (hydrogen acceptors) and blue region, which is a positive electrostatic potential (hydrogen donor). The intercontacts and their quantification was done using visualization of the Hirshfeld surfaces and 2D fingerprint plots (Fig. 8). The fingerprint plot for **3f** shows that the major contributions are from H….H interactions with 33.6% while the O….H interactions contribute 17.4%.

https://doi.org/10.1016/j.heliyon.2019.e01131

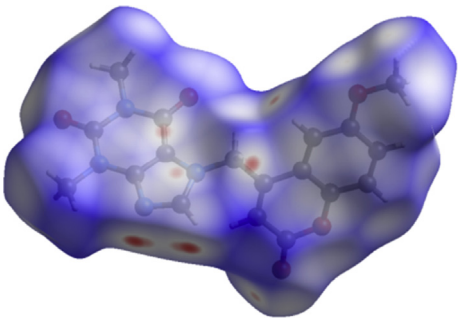

Fig. 6. Dnorm mapped on Hirshfeld surface for visualizing the intercontacts of the complex. Color scaled in between -0.1464 to +1.2778 au for compound **3f**.

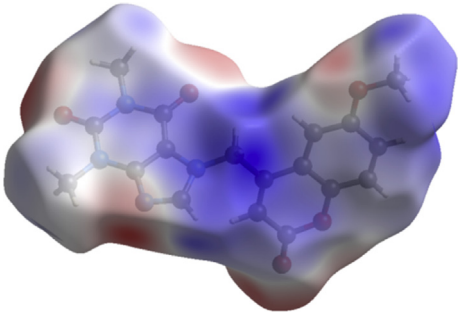

Fig. 7. Electrostatic potential mapped on Hirshfeld surface (different orientation) with -0.0889 to +0.0587au. Blue region corresponds to positive electrostatic potential and red region to negative electrostatic potential for compound **3f**.

3. Experimental

3.1. Materials and methods

All the chemicals purchased were of analytical grade and used without further purification. Melting points were obtained with the open capillary method on a Buchi apparatus and are uncorrected. IR spectra were recorded using KBr pellets on a Nicolet 5700 FT-IR instrument. ^{1}H and ^{13}C NMR spectra were recorded on JEOL 400MHz and Bruker 400 MHz Spectrometer using DMSO-d_6 and $CDCl_3$ as solvents and TMS as internal standard reference and chemical shifts were reported as δ values (ppm). Shimadzu GCMSQP2010S was used to record the Mass spectra. Hereaus CHN rapid analyzer was used to record the elemental analysis. TLC was used to check the purity of the compounds.

3.1.1. Synthesis of coumarin-purine derivatives (3a-3j)

3.1.1.1. MW method

A mixture of 4-methylbromocoumarins (0.01 mol) with purine (0.01 mol) and K_2CO_3 (0.02) in 10 ml MW vial with 5 ml of dry acetone was run into MW irradiator at 50 °C for 5−9 min and cooled. The progress of the reaction was examined by thin

https://doi.org/10.1016/j.heliyon.2019.e01131

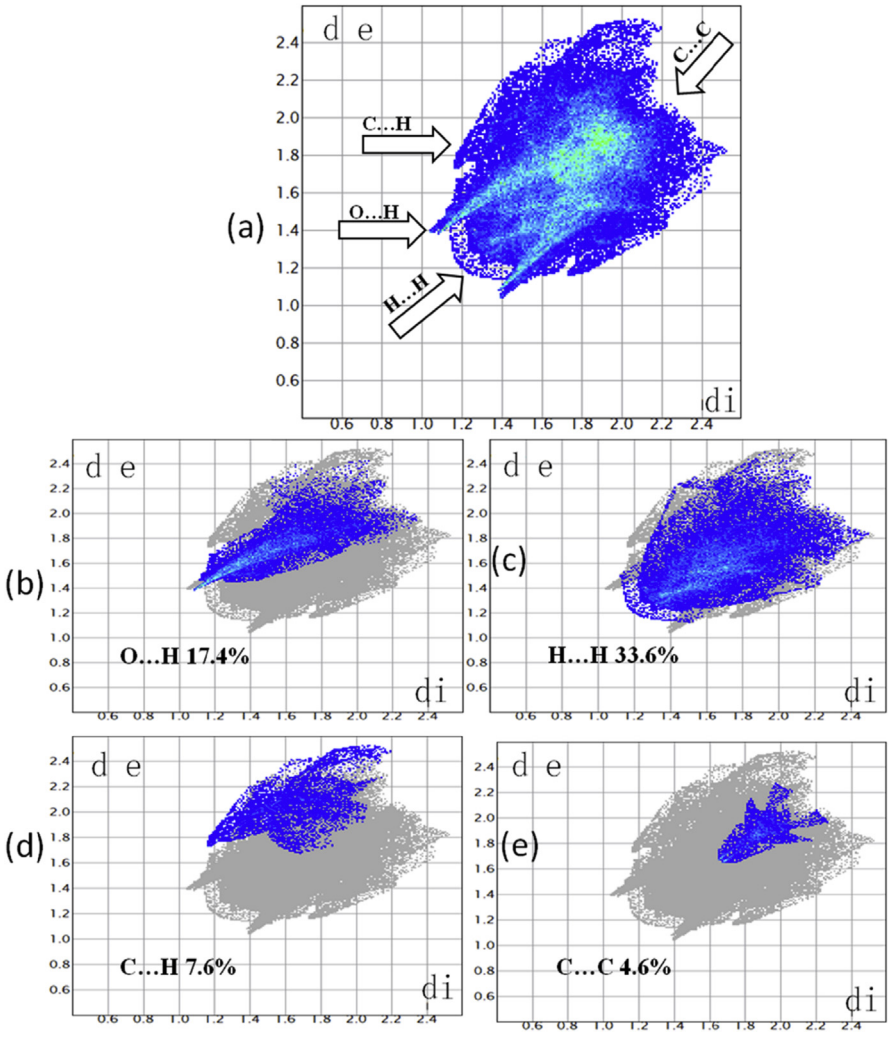

Fig. 8. Fingerprint plots: Hirshfeld surfaces and 2D fingerprint plots of compound and outline of the full fingerprint is shown in grey (a) and other intercontacts from (b−e). di is the closest internal distance from a given point on the Hirshfeld surface and de is the closest external contacts for compound **3f.**

layer chromatography (TLC). The reaction mixture was quenched to the crushed ice; the solid product obtained was filtered and washed with water.

3.1.1.2. Conventional method

A mixture of substituted 4-methylbromocoumarins (0.01 mol) with purine (0.01 mol) and K_2CO_3 (0.02) in acetone for 4−6 h. The completion of the reaction was confirmed by thin layer chromatography (TLC) and followed the procedure as prescribed in MW method.

3.1.2. Single crystal X-ray diffraction studies

Single crystal X-ray diffraction data for the compound was collected at 296(2) K on a Bruker APEX-II CCD diffractometer using graphite monochromater Mo Kα (λ =

https://doi.org/10.1016/j.heliyon.2019.e01131

0.71073 Å). The structure was solved using OLEX2 [31] with SHELXS by direct methods. The structure was refined by full-matrix least-squares minimization with SHELXL [32]. Non-hydrogen atom positions were found and refined anisotropically. Whereas, hydrogen atoms were positioned geometrically and treated as riding atoms where C−H = 0.93 Å with Uiso (H) = 1.2 Ueq (C) for aromatic carbon atoms and C−H = 0.96 Å with Uiso (H) = 1.5 Ueq (C) for methyl carbon atoms [33].

3.1.3. Computational details

The theoretical calculations of compound 3f has been performed using DFT-B3LYP/6-311G++ (d, p) basis set, using the Gaussian 09W [34] and Gauss view 5 [35] program. The optimizations of molecular structure in the ground state [36] and bond length and bond angle calculations for compound 3f has been carried out by using B3LYP/6−31 + G method. The energies of HOMO and LUMO electronic properties were being recognized by DFT approach.

3.1.4. Biological assay

3.1.4.1. Evaluation of antioxidant activity by DPPH radical scavenging activity

The antioxidant activity of the synthesized compounds was measured on the basis of the free radical scavenging activity by the DPPH (1, 1- diphenyl 2-picrylhydrazyl) method. The stock solution of DPPH· was prepared by dissolving 3.9432 mg DPPH in 100 mL of methanol (0.1 mM) and stored at 4 °C until use. 2 ml of DPPH solution was mixed with 1 mL of different concentrations (20−100 $\mu g mL^{-1}$) of the compounds. Ascorbic acid (100 $\mu g mL^{-1}$) was used as the reference standard. Mixture of 1 mL distilled water and 2 mL DPPH solution was used as the control. The reaction mixture was mixed and incubated at room temperature in the dark for 30 min. The absorbance was recorded spectrophotometrically at 517 nm.

The antioxidant activity of the compounds was estimated based on the percentage of DPPH radical scavenged as the following equation:

$$\text{Scavenging effect } \% = \frac{[\text{control absorbance} - \text{sample absorbance}]}{\text{Control absorbance}} \times 100$$

3.1.4.2. DNA cleavage studies by electrophoresis analysis

3.1.4.2.1. Sample preparation

Calf-Thymus DNA (CT-DNA) was procured from Merck. A DNA stock solution was prepared by diluting the CT-DNA in TE buffer. The test compounds (5 mM)

https://doi.org/10.1016/j.heliyon.2019.e01131

were dissolved in DMSO and added separately to the 10 ml of CT-DNA and then incubated at 37 °C for 2 h.

3.1.4.2.2. Agarose gel electrophoresis

The cleavage of Calf-Thymus DNA (CT-DNA) by the products was analyzed using an agarose gel electrophoresis method. The gel electrophoresis was performed on 1% agarose the wells were loaded with 10 μL of DNA, 5 mm of the test compound and 10 μL of the tracking dye. Electrophoresis was performed at 50 V for 45 min. The gel was observed under UV trans illuminator and DNA bands of test samples were with that of untreated control and a marker was used to examine the molecular weight.

3.1.5. Biological evaluation

3.1.5.1. In vitro antioxidant activity

In the present investigation of different concentrations of coumarin-purine derivatives were subjected to DPPH free radical scavenging assay with standard ascorbic acid. From the results it is clear that the substitutions on the coumarin ring enhances the radical scavenging activity, especially the −OH functional group is favorable for increase in the activity. The compound **3i,** shows the most excellent DPPH scavenging activity with a −OH substitution at C7 of coumarin ring. The compound **3f,** has shown good scavenging activity with $-OCH_3$, substitution at C6 of coumarin ring. Further the compounds **3j** and **3e** also were found to be good scavengers with the substitutions 6-*tert butyl* and 3,5-dimethyl of the coumarin ring. The remaining compounds **3a, 3b, 3c, 3d, 3g** and **3h** have shown good to moderate scavenging activity. However, the radical scavenging activity is depending on the functional group and position of the desired compounds and the results are given in Table 4.

3.1.5.2. Electrophoresis analysis

In order, to synthesize potent drugs it is essential to know the ability of compound to cleave/bind DNA. Therefore, the synthesized compounds **(3a−3j)** were subjected to CT-DNA cleavage assay using an agarose gel electrophoresis method, and the results are presented in Fig. 9. The control sample was maintained and the bands appeared with test compounds were compared with that of bands appeared in the control sample. It was observed that compound **3j** did cleave the DNA more efficiently, as no traces of DNA were found. Immobilization of DNA may be due to the binding activity of compounds that observed in the wells loaded with compounds (**3a, 3b, 3c, 3d, 3g, 3h and 3i**). Whereas shearing of DNA was observed with the sample **3e.** No changes was recorded in the band of **3f** treated compound when compared to the control indicating that the test compound **(3f)** was found to be

https://doi.org/10.1016/j.heliyon.2019.e01131

Table 4. *In-vitro* antioxidant screening results by DPPH free radical scavenging assay.

Comp code	Conc. μgmL^{-1}	Conc. μM	Radical scavenging activity (%)
	20	113.55	40.36 ± 0.75
	40	227.12	58.60 ± .916
Ascorbic acid	60	340.67	75.40 ± 2.12
	80	454.23	85.23 ± 1.21
	100	567.79	95.15 ± 1.91
	20	56.76	23.50 ± 1.01
	40	113.52	31.55 ± 1.08
3a**	60	170.29	46.98 ± 1.68
	80	227.05	60.62 ± 0.85
	100	283.81	71.69 ± 1.04
	20	56.76	15.56 ± 0.95
	40	113.52	23.35 ± 2.00
3b**	60	170.29	32.39 ± 0.87
	80	227.05	44.61 ± 3.93
	100	283.81	57.14 ± 1.74
	20	51.49	23.02 ± 1.68
	40	102.99	31.72 ± 1.64
3c**	60	154.48	42.94 ± 1.74
	80	205.98	58.43 ± 1.29
	100	257.48	70.82 ± 0.73
	20	51.49	20.38 ± 0.96
	40	102.99	29.39 ± 1.14
3d**	60	154.48	41.61 ± 0.82
	80	205.98	56.43 ± 0.71
	100	257.48	63.48 ± 2.06
	20	54.59	27.19 ± 1.22
	40	109.17	32.55 ± 2.01
3e**	60	163.77	49.65 ± 0.66
	80	218.35	61.62 ± 0.85
	100	272.94	72.69 ± 1.24
	20	54.29	28.08 ± 0.19
	40	108.59	39.53 ± 1.22
3f**	60	162.89	51.51 ± 0.92
	80	217.19	62.90 ± 2.69
	100	271.49	79.37 ± 1.00
	20	53.65	11.37 ± 0.95

(*continued on next page*)

https://doi.org/10.1016/j.heliyon.2019.e01131

Table 4. (*Continued*)

Comp code	Conc. μgmL^{-1}	Conc. μM	Radical scavenging activity (%)
	40	107.30	18.22 ± 2.05
3g**	60	160.96	27.32 ± 1.48
	80	214.61	35.89 ± 1.52
	100	268.31	53.65 ± 0.86
	20	47.93	14.30 ± 1.58
	40	95.87	22.35 ± 1.01
3h**	60	143.81	34.39 ± 1.07
	80	191.74	47.28 ± 2.25
	100	239.68	59.43 ± 0.97
	20	56.45	30.09 ± 1.16
	40	112.89	43.90 ± 2.39
3i**	60	169.38	62.51 ± 0.92
	80	225.78	75.24 ± 1.78
	100	282.23	87.04 ± 1.54
	20	50.71	30.13 ± 1.62
	40	101.41	38.87 ± 1.47
3j**	60	152.12	51.18 ± 2.19
	80	202.82	65.24 ± 1.63
	100	253.53	81.71 ± 1.51

Values are expressed as mean ± SD, n = 3 and.
** Correlation is significant at the 0.01 level.

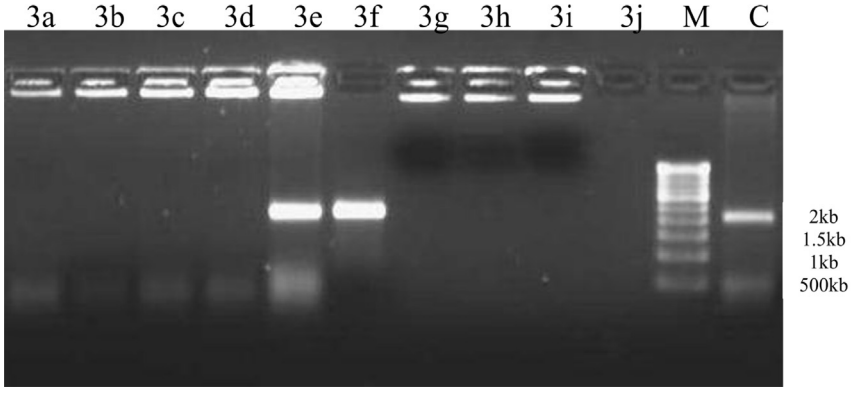

Fig. 9. CT-DNA cleavage study using agarose gel electrophoresis. Lane M: standard DNA marker, Lane C: control DNA (untreated sample), Lane 3a: DNA + 3a, Lane 3b: DNA + 3b, Lane 3c: DNA + 3c, Lane 3d: DNA + 3d, Lane 3e: DNA + 3e, Lane 3f: DNA + 3f, Lane 3g: DNA + 3g, Lane 3h: DNA + 3h, Lane 3i: DNA + 3i, Lane 3j: DNA + 3j.

https://doi.org/10.1016/j.heliyon.2019.e01131

inactive to cleave or bind to the DNA. The results of present study conclude that the DNA cleavage or binding activity of the compound depends upon the position of the functional group. The substituent like *-tert butyl* (electron donating), at C-6 position of coumarin is most favorable. Other substituent's C6-CH_3, C7-CH_3, 5,6-benzo, 7,8-benzo, C6-Cl, C6-Br and C7-OH were shown binding activity to DNA.

4. Conclusions

The title compounds **(3a-3j)** were synthesized under microwave irradiation method. The microwave approach has been demonstrated to be extremely fast, with enhanced reaction rate and shorter time, providing desired compounds in good to excellent yields and in high purity as compared to the conventional method. X-ray structure of the compound **3f** crystallized under a monoclinic system with the space group $P2_1/n$. The DFT results showed that geometry optimization calculations confirm the experimental results. Hirshfeld surface analysis and fingerprint plots give the nature of intermolecular interactions and percentage contribution from each individual contact. *In vitro* anti-oxidant activity of compound **3i**, was found to exhibit excellent activity due to the presence of hydroxyl (−OH) group by using standard ascorbic acid. The compound **3j**, is capable to cleave DNA completely.

Declarations

Author contribution statement

Sumitra Mangasuli: Conceived and designed the experiments; Performed the experiments; Analyzed and interpreted the data; Wrote the paper.

Praveen Managutti: Conceived and designed the experiments; Analyzed and interpreted the data; Wrote the paper.

Kallappa M. Hosamani: Conceived and designed the experiments; analyzed and interpreted the data.

Funding statement

This research did not receive any specific grant from funding agencies in the public, commercial, or not-for-profit sectors.

Competing interest statement

The authors declare no conflict of interest.

https://doi.org/10.1016/j.heliyon.2019.e01131

Additional information

The spectral data of synthesized compounds (**3a-3j**) are available under DOI: https://doi.org/10.1016/j.ejmech.2018.01.025. Crystallographic data had been deposited with the Cambridge Crystallographic Data Centre as supplementary publication for the compound (**3f**) with CCDC No. 1848347.

Supplementary content related to this article has been published online at https://doi.org/10.1016/j.heliyon.2019.e01131.

Acknowledgements

The authors acknowledge University Scientific Instrumentation Centre (USIC), Karnatak University, Dharwad for carrying out the spectral analyses.

References

[1] J. Hamelin, J.P. Bazureau, F.T. Boullet, in: A. Loupy (Ed.), Microwaves in Organic Chemisry, second ed., Wiley-VCH, Weinheim, Germany, 2003, p. 253. Ch. 8.

[2] A. de la Hoz, A. Diaz-Ortizand, A. Moreno, Microwaves in organic synthesis. Thermal, and non-thermal microwave effects, Chem. Soc. Rev. 24 (2005) 164−178.

[3] C.O. Kappe, Microwave dielectric heating in synthetic organic chemistry, Chem. Soc. Rev. 37 (2008) 1127.

[4] R. Sarma, D. Prajapati, Microwave-promoted efficient synthesis of dihydroquinazolines, Green Chem. 13 (2011) 718−722.

[5] R. Gedye, F. Smith, K. Westaway, H. Ali, Fundamentals, representative applications and future perspectives of green chemistry: a short review, Tetrahedron Lett. 27 (2016) 279−282.

[6] B.L. Hayes, Recent advances in microwave assisted synthesis, Aldrichim. Acta 37 (2) (2004) 66−76.

[7] D. Bogdal, Microwave Assisted Organic Synthesis, Elsevier Publications, UK, 2005, p. 13.

[8] V. Santagada, F. Frecentese, E. Perissutti, F. Fiorino, B. Severino, G. Caliendo, Microwave assisted synthesis: a new technology in drug discovery, Mini Rev. Med. Chem. 9 (2009) 340−358.

[9] M. Nuchter, B. Ondruschka, W. Bonrath, A. Gum, Microwave assisted synthesis − a critical technology overview, Green Chem. 6 (2004) 128−141.

[10] C.O. Kappe, B. Pieber, D. Dallinger, Microwave effects in organic synthesis: myth or reality? Angew. Chem. Int. Ed. 52 (2013) 1088−1094.

[11] J.C. Fonseca, M.A. Barbosa, I.C.A. Silva, J.M. Duarte-Almeida, A.H.F. Castro, L.A.R. dos Santos Lima, Antioxidant and allelopathic activities of *Smilax brasiliensis* Sprengel (Smilacaceae), South Afr. J. Bot. 111 (2017) 336−340.

[12] M. Roussaki, C.A. Kontogiorgis, D. Hadjipavlou-Litina, S. Hamilakis, A. Detsi, A novel synthesis of 3-aryl coumarins and evaluation of their antioxidant and lipoxygenase Inhibitory activity, Bioorg. Med. Chem. Lett 20 (2010) 3889−3892.

[13] R. Kenchappa, Y.D. Bodke, A. Chandrashekar, M.A. Sindhe, S.K. Peethambar, Synthesis of coumarin derivatives containing pyrazole and indenone rings as potent antioxidant and antihyperglycemic agents, Arab. J. Chem. 10 (2017) S3895−S3906.

[14] G. Padilha, P.T. Birmann, M. Domingues, T.S. Kaufman, L. Savegnago, C.C. Silveira, Convenient Michael addition/b-elimination approach to the synthesis of 4-benzyl- and 4-aryl-selenyl coumarins using diselenides as selenium sources, Tetrahedron Lett. 58 (2017) 985−990.

[15] M. Traykova, I. Kostova, Coumarin derivatives and antioxidative stress, Int. J. Pharmacol. 1 (2005) 29−32.

[16] K.C. Fylaktakidou, D.J. Hadjipavlou-Litina, K.E. Litinas, D.N. Nikolaides, Natural and synthetic coumarin derivatives with anti-inflammatory/antioxidant activities, Curr. Pharmaceut. Des. 10 (2004) 3813−3833.

[17] V. Thomas, D. Giles, G.P.M. Basavarajaswamy, A.K. Das, A. Patel, Coumarin derivatives as anti-inflammatory and anticancer agents, Anti Cancer Agents Med. Chem. 17 (3) (2017) 415−423.

[18] D.J. Hadjipavlou-Litina, K.E. Litinas, C. Kontogiorgis, The anti-inflammatory effect of coumarin and its derivatives, Anti-Inflammatory Anti-Allergy Agents Med. Chem. 6 (4) (2007) 293−306.

[19] Y. Donglei, M. Suzuki, L. Xie, S.L. Morris-Natschke, L. Kuo-Hsiung, Recent progress in the development of coumarin derivatives as potent anti-HIVA gents, Med. Res. Rev. 23 (3) (2003) 322−345.

[20] R.S. Keri, B.S. Sasidhar, B.M. Nagaraja, M.A. Santos, Recent progress in the drug development of coumarin derivatives as potent antituberculosis agents, Eur. J. Med. Chem. 100 (2015) 257−269.

 https://doi.org/10.1016/j.heliyon.2019.e01131

[21] S.N. Mangasuli, K.M. Hosamani, P. Satapute, S.D. Joshi, Synthesis, molecular docking studies and biological evaluation of potent coumarin−carbonodithioate hybrids via microwave irradiation, Chem. Data Collect. 15−16 (2018) 115−125.

[22] S.A. Morsy, A.A. Farahat, M.N.A. Nasr, A.S. Tantawy, Synthesis, molecular modeling and anticancer activity of new coumarin containing compounds, Saudi Pharmaceut. J. (2017).

[23] (a)S.N. Mangasuli, K.M. Hosamani, P. Managutti, D.A. Barretto, S.D. Joshi, Synthesis, molecular docking studies and biological evaluation of potent coumarin-thiazolidinone hybrids: an approach to microwave synthesis, Chem. Data Collect. 17−18 (2018) 327−338;
(b)D.J. Hadjipavlou-Litina, K.E. Litinas, C. Kontogiorgis, The anti-inflammatory effect of coumarin and its derivatives, Anti-Inflammatory Anti-Allergy Agents Med. Chem. 6 (4) (2007) 293−306.

[24] L. Huang, X. Yuan, D. Yu, K.H. Lee, C.H. Chen, Mechanism of action and resistant profile of anti-HIV-1 coumarin derivatives, Virology 332 (2) (2005) 623−628.

[25] Y. Yang, Q.-W. Liu, Y. Shi, Z.-G. Song, Y.-H. Jin, Z.-Q. Liu, Design and synthesis of coumarin-3-acylamino derivatives to scavenge radicals and to protect DNA, Eur. J. Med. Chem. 84 (2014) 1−7.

[26] D.R. Vianna, G. Bubols, G. Meirelles, B.V. Silva, A.D. Rocha, M. Lanznaster, J.M. Monserrat, S.C. Garcia, G.V. Poser, V.L. Eifler-Lima, Evaluation of the antioxidant capacity of synthesized coumarins, Int. J. Mol. Sci. 13 (2012) 7260−7270.

[27] S. Azam, N. Hadi, N.U. Khan, S.M. Hadi, Antioxidant and prooxidant properties of caffeine, theobromine and xanthine, Med. Sci. Monit. 29 (9) (2003) BR325−BR330.

[28] S.N. Mangasuli, K.M. Hosamani, H.C. Devarajegowda, M.M. Kurjogi, S.D. Joshi, Synthesis of coumarin-theophylline hybrids as a new class of anti-tubercular and anti-microbial agents, Eur. J. Med. Chem. 146 (2018) 747−756.

[29] D.S. Reddy, K.M. Hosamani, H.C. Devarajegowda, M.M. Kurjogi, A facile synthesis and evaluation of new biomolecule-based coumarin−thiazoline hybrids as potent anti-tubercular agents with cytotoxicity, DNA cleavage and X-ray studies, RSC Adv. 5 (2015) 64566−64581.

[30] S. Koparde, K.M. Hosamani, D.A. Barretto, S.D. Joshi, Microwave synthesis of coumarin-maltol hybrids as potent antitumor and anti-microbial drugs: an

https://doi.org/10.1016/j.heliyon.2019.e01131

approach to molecular docking and DNA cleavage studies, Chem. Data Collect. 15–16 (2018) 41–53.

[31] O.V. Dolomanov, L.J. Bourhis, R.J. Gildea, J.A.K. Howard, H. Puschmann, OLEX2: a complete structure solution, refinement and analysis program, J. Appl. Crystallogr. 42 (2009) 339–341.

[32] G.M. Sheldrick, A short history of SHELX, ActaCryst A64 (2008) 112–122.

[33] M.N. Arshad, A. Bibi, T. Mahmood, A.M. Asiri, K. Ayub, Synthesis, crystal structures and spectroscopic properties of triazine-based hydrazone derivatives; a comparative experimental-theoretical study, Molecules 20 (4) (2015) 5851–5874.

[34] M.J. Frisch, G.W. Trucks, H.B. Schlegel, G.E. Scuseria, M.A. Robb, J.R. Cheeseman, G. Scalmani, V. Barone, B. Mennucci, G.A. Petersson, H. Nakatsuji, M. Caricato, X. Li, H.P. Hratchian, A.F. Izmaylov, J. Bloino, G. Zheng, J.L. Sonnenberg, M. Hada, M. Ehara, K. Toyota, R. Fukuda, J. Hasegawa, M. Ishida, T. Nakajima, Y. Honda, O. Kitao, H. Nakai, T. Vreven, J.A. Montgomery, J.E. Peralta, F. Ogliaro, M. Bearpark, J.J. Heyd, E. Brothers, K.N. Kudin, V.N. Staroverov, R. Kobayashi, J. Normand, K. Raghavachari, A. Rendell, J.C. Burant, S.S. Iyengar, J. Tomasi, M. Cossi, N. Rega, J.M. Millam, M. Klene, J.E. Knox, J.B. Cross, V. Bakken, C. Adamo, J. Jaramillo, R. Gomperts, R.E. Stratmann, O. Yazyev, A.J. Austin, R. Cammi, C. Pomelli, J.W. Ochterski, R.L. Martin, K. Morokuma, V.G. Zakrzewski, G.A. Voth, P. Salvador, J.J. Dannenberg, S. Dapprich, A.D. Daniels, Farkas, J.B. Foresman, J.V. Ortiz, J. Cioslowski, D.J. Fox, Gaussian 09, Revision B.01, Gaussian, Inc., Wallingford CT, 2010.

[35] R. Dennington, T. Keith, J. Millam, Gauss View Version 5, Semichem Inc., Shawnee Mission KS, 2009.

[36] A.M. K∈oster, M. Leboeuf, D.R. Salahub, Molecular electrostatic potentials from density functional theory, in: S.M. Jane, S. Kalidas (Eds.), Theoretical and Computational Chemistry, Elsevier, 1996, pp. 105–142.

https://doi.org/10.1016/j.heliyon.2019.e01131